Available online on 15.09.2022 at http://jddtonline.info

Journal of Drug Delivery and Therapeutics

Open Access to Pharmaceutical and Medical Research



*Open Access Full Text Article*

Research Article

# ADMET informatics of Plant Derived n-Hexadecanoic Acid (Palmitic Acid) from ethyl acetate fraction of *Moringa oleifera* leaf extract

Krishnaveni K.[1], Murugan M.[2], Kalaimathi RV.[2], Basha AN.[1], Pallan GA.[1], Kandeepan C.[1], Senthilkumar N.[3], Mathialagan B.[4], Ramya S.[4], Jayakumararaj R.*[5], Loganathan T.[6], Pandiarajan G.[7], Kaliraj P.[8], Ram Chand Dhakar[9]

[1] *PG & Research Department of Zoology, Arulmigu Palaniandavar College of Arts & Culture, Palani – 624601, TN, India*
[2] *Department of Zoology, GTN Arts & Science College, Dindigul - 624005, TN, India*
[3] *Institute of Forest Genetics & Tree Breeding* (IFGTB), *Indian Council of Forestry Research & Education (ICFRE), Coimbatore – 641002, TN, India*
[4] *PG Department of Zoology, Yadava College (Men), Thiruppalai - 625014, Madurai, TN, India*
[5] *Department of Botany, Government Arts College, Melur – 625106, Madurai District, TN, India*
[6] *Department of Plant Biology & Plant Biotechnology, LN Government College (A), Ponneri, TN, India*
[7] *Department of Botany, Sri S Ramasamy Naidu Memorial College (A), Sattur - 626203 TN, India*
[8] *Department of Zoology, Sri S Ramasamy Naidu Memorial College (A), Sattur - 626203 TN, India*
[9] *Hospital Pharmacy, SRG Hospital & Medical College Jhalawar-326001, Rajasthan, India*

Article Info:

Article History:

Received 26 July 2022
Reviewed 01 Sep 2022
Accepted 08 Sep 2022
Published 15 Sep 2022

Cite this article as:

Krishnaveni K, Murugan M, Kalaimathi RV, Basha AN, Pallan GA, Kandeepan C, Senthilkumar N, Mathialagan B, Ramya S, Jayakumararaj R, Loganathan T, Pandiarajan G, Kaliraj P, Dhakar RC, ADMET informatics of Plant Derived n-Hexadecanoic Acid (Palmitic Acid) from ethyl acetate fraction of *Moringa oleifera* leaf extract, Journal of Drug Delivery and Therapeutics. 2022; 12(5):132-145

*DOI: http://dx.doi.org/10.22270/jddt.v12i5.5605*

*Address for Correspondence:

Jayakumararaj R., Department of Botany, Government Arts College, Melur – 625106, Madurai District, TN, India

## Abstract

Palmitic Acid (PA) is known to exert multiple fundamental biological functions at cellular and tissue levels and its steady concentration is guaranteed by its endogenous synthesis by DNL. PA has been for a long time negatively represented for its detrimental health effects tailing its essential physiological attributes. PA has been portrayed to serve as a signalling molecule regulating the progression and development of many diseases at molecular level. Controversial data on the association of dietary PA with detrimental health effects has been related to several parameters such as fatty acid/ macronutrient imbalance by altered lipid metabolism, positive energy balance, excessive intake of carbohydrates, imbalance of dietary PA/PUFA, physiopathological conditions, presence of enhanced DNL and sedentary lifestyle. This may result in dyslipidemia, hyperglycemia, increased ectopic fat accumulation and increased inflammatory tone indicating that clear understanding of system based PA metabolism is still lacking. In the present study an attempt has been made to bring out the absorption, distribution, metabolism, elimination and toxicity profile of PA. Results are expected to have some implications in elucidating the molecular mechanisms that regulates pathophysiological events involved in hyperglycemia/ hyperlipidemia-induced complications associated with diabesity and CVD. Besides it may provide a better understanding to identify key molecular targets for therapeutic management of PA induced metabolic disorders.

**Keywords:** *Moringa oleifera*; MOLE; Bioactive Secondary Metabolites; ADME/Tox; Natural Products (NPs); PBNPs; PDHA; n-Hexadecanoic Acid (nHDA); Palmitic Acid (PA)

## INTRODUCTION

Palmitic acid, (PA) is the most common saturated fatty acid found in animals, plants and microorganisms. It's C:D (Total number of carbon atoms to the total number of carbon-carbon double-bonds) is 16:0[1]. It is a major component of oil from fruits of oil palms (palm-oil), 44% of total fats. Meat, cheeses, butter, and other dairy products also contain higher amounts of palmitic acid (50–60% of total fats)[2]. Chemically, palmitates are salts and esters of PA, on the other hand palmitate is anion form of PA at a pH of 7.4. It has been demonstrated that PA represents 20–30% of total fatty acids (FA) in membrane phospholipids (PL), and adipose triacylglycerols (TAG)[3], and can be provided in the diet or synthesized endogenously via *de novo* lipogenesis (DNL).

PA has been for long time negatively depicted for its putative detrimental health effects, shadowing its multiple biochemical, metabolic and physiological activities[3]. It has been established that the level of PA content is controlled by a well-defined concentration, and changes in its intake doesn't influence tissue concentration as exogenous source is counter balanced by the endogenous biosynthesised PA. Disruption of PA homeostatic balance, implicated in different physio-

pathological conditions is often related to endogenous synthesis of PA, irrespective of its dietary intake[4]. It has been pointed out that increasing dietary PA decreases fat oxidation and daily energy expenditure in the system[5]. However, overproduction of PA by DNL, activated by physio-pathological conditions and chronic nutritional imbalance, leads to a systemic inflammatory response (SIR) and metabolic dysregulation, resulting in dyslipidemia, insulin resistance and dysregulated fat deposition and distribution[6]. Further, increase in cellular concentration of PA impairs endothelial progenitor cells and bone marrow-derived progenitor cell bioavailability[7]. PA induces central leptin resistance and impairs hepatic glucose and lipid metabolism[8]. It dysregulates the Hippo-YAP pathway and inhibits angiogenesis by inducing mitochondrial damage and activating the cytosolic DNA sensor cGAS-STING-IRF3 signalling mechanism[9]. Emerging evidence shows that PA serves as an intracellular signalling molecule regulating the progression and development of many diseases at the molecular level[10]. Studies depict that high-fat diet (HFD)-induced obesity is associated with increased cancer risk. PA increases invasiveness of pancreatic cancer cells AsPC-1 through TLR4/ROS/NF-kappaB/MMP-9 signalling pathway[11]. Further, PA impairs hepatocellular carcinoma development by modulating membrane fluidity and glucose metabolism[12]. PA has been reported to induce neurotoxicity and gliatoxicity in SH-SY5Y human neuroblastoma and T98G human glioblastoma cells[13]. PA reduces the autophagic flux in hypothalamic neurons by impairing autophagosome-lysosome fusion and endolysosomal dynamics[14]. It has been indicated that, long-term feeding with HFD increases the concentration of PA in hypothalamus; hypothalamic neuronal cells, up on exposure to PA inhibits autophagic flux from the synthesis of the autophagosomes, up to their lysosomal fusion and degradation. However, mechanism by which PA impairs autophagy in hypothalamic neurons remains unknown. Further, impaired autophagy in hypothalamic neurons promotes obesity, which suggests that a balanced autophagy is required to inhibit malignant transformation and results in tumor initiation, progression, and/ or response to therapy of obesity-related cancers[15]. *Moringa oleifera* leaf is a low cost food material that remains as excellent source of proteins, essential and non-essential amino acids, lipids, sugars, essential fatty acids, vitamin precursors, and mineral, as well as organic acid, terpenoids, alkaloids, steroids, and phenolic compounds. Moringa leaf has been commonly used as therapeutic food to prevent hypertension, hypercholesterolemia, atherosclerosis, diabetes, cancer and malnutrition among economically poor section of people in developing countries[16-30]. In recent years, combinatorial chemistry and high-throughput screening have significantly increased the number of compounds for which early data on absorption, distribution, metabolism, excretion (ADME) and toxicity (T) are needed, which has in turn driven the development of a variety of medium and high-throughput *in vitro* ADMET screens for drug development and design with deeper dimension ad interim maintain high degree of precision taking into account time and cost economics[30-42]. In the current framework of the available experimental evidences related to PA, it is clear that there exists a knowledge gap in terms of its biomedical application due to the dearth of ADMET data and preclinical trails that hampers exploitation of PA by pharma-industries on commercial basis.

## MATERIALS AND METHODS

### *In silico* Drug-Likeliness and Bioactivity Prediction

The drug likeliness and bioactivity of selected molecule was analyzed using the Molinspiration server (http://www.molinspiration.com). Molinspiration tool is cheminformatics software that provides molecular properties as well as bioactivity prediction of compounds[43]. In Molinspiration-based drug-likeness analysis, there are two important factors, including the lipophilicity level (log P) and polar surface area (PSA) directly associated with the pharmacokinetic properties (PK) of the compounds[44]. In Molinspiration-based bioactivity analysis, the calculation of the bioactivity score of compounds toward GPCR ligands, ion channel modulators, kinase inhibitors, nuclear receptor ligands, protease inhibitors, and other enzyme targets were analyzed by Bayesian statistics[43]. This was carried out for G protein-coupled receptors (GPCR), ion channels, kinases, nuclear hormone receptors, proteases, and other enzymes (RdRp), are the major drug targets of most of the drugs[45].

### *In silico* ADMET Analysis

**SwissADME**: is a Web tool that gives free access to a pool of fast yet robust predictive models for physicochemical properties, pharmacokinetics, druglikeness and medicinal chemistry friendliness, among which in-house proficient methods such as iLOGP (a physics-based model for lipophilicity) or the BOILED-Egg (an intuitive graphical classification model for gastrointestinal absorption and brain access). It is the first online tool that enables ADME-related calculation for multiple molecules, allowing chemical library analysis and efficient lead optimization[46]. PK properties, such as Absorption, Distribution, Metabolism, Excretion, and Toxicity (ADMET), of fatty acids were predicted using admerSAR v2.0 server (http://lmmd.ecust.edu.cn/admetsar2/) and The admerSAR server is an open-source computational tool for prediction of ADMET properties of compounds, which makes it a practical platform for drug discovery and other pharmacological research[47]. In ADMET analysis, absorption (A) of good drugs depends on factors such as membrane permeability[48] [designated by colon cancer cell line (Caco-2)], human intestinal absorption (HIA)[49], and status of either P-glycoprotein substrate or inhibitor[50]. Distribution (D) of drugs mainly depends on the ability to cross blood-brain barrier (BBB)[51]. The metabolism (M) of drugs is calculated by the CYP, MATE1, and OATP1B1-OATP1B3 models[52]. Excretion (E) of drugs is estimated based on the renal OCT substrate. Toxicity (T) of drugs is predicted on Human Ether-A-Go-Go related gene inhibition, carcinogenic status, mutagenic status, and acute oral toxicity[53].

### vNN model building and analysis

vNN method was used to calculate the similarity distance between molecules in terms of their structure, and uses a distance threshold to define a domain of applicability to ensures that the predictions generated are reliable. vNN models can be built keeping quantitative structure–activity relationship (**QSAR**) models up-to-date to maintain their performance levels. Performance characteristics of the models are comparable, and often superior to those of other more elaborate model.[54-61] One of the most widely used measures of similarity distance between two small molecules is Tanimoto distance, d, which is defined as:

$$d = 1 - \frac{n(\mathrm{P} \cap \mathrm{Q})}{n(P) + n(Q) - (\mathrm{P} \cap \mathrm{Q})}$$

where n(P∩Q) is number of features common to molecules p and q, and n(P) and n(Q) are the total numbers of features for molecules p and q, respectively. The predicted biological activity y is given by a weighted across structurally similar neighbours:

$$y = \frac{\sum_{i=1yie}^{v} -(di/h)^2}{\sum_{i=1e}^{v} -(di/h)^2} \; di \leq d0$$

where $d_i$ denotes Tanimoto distance between a query molecule for which a prediction is made and a molecule i of the training set; $d_0$ is a Tanimoto-distance threshold, beyond which two molecules are no longer considered to be sufficiently similar to be included in the average; $y_i$ is the experimentally measured activity of molecule i; v denotes the total number of molecules in the training set that satisfies the condition $d_i \leq d_0$; and h is a smoothing factor, which dampens the distance penalty. Values of h and $d_0$ are determined from cross-validation studies. To identify structurally similar compounds, Accelrys Extended-Connectivity FingerPrints with a diameter of four chemical bonds (ECFP4) were used[54-61].

**Model Validation**

A 10-fold cross-validation (CV) procedure was used to validate new models and to determine the values of smoothing factor h and Tanimoto distance $d_0$. In this procedure, data was randomly divided into 10 sets, and used 9 to develop the model and 10th to validate it, this process was repeated 10 times, leaving each set of molecules out once.

**Performance Measures**

Following metrics were used to assess model performance. (1) sensitivity measures a model's ability to correctly detect true positives, (2) specificity measures a model's ability to detect true negatives, (3) accuracy measures a model's ability to make correct predictions and (4) kappa compares the probability of correct predictions to the probability of correct predictions by chance (its value ranges from +1 (perfect agreement between model prediction and experiment) to –1 (complete disagreement), with 0 indicating no agreement beyond that expected by chance).

$$\text{sensitivity} = \frac{\text{TP}}{\text{TP} + \text{FN}}$$

$$\text{specificity} = \frac{\text{TN}}{\text{FP} + \text{TN}}$$

$$\text{accuracy} = \frac{\text{TP} + \text{TN}}{\text{TP} + \text{TN} + \text{FP} + \text{FN}}$$

$$kappa = \frac{\text{accuracy} - \Pr(\text{e})}{1 - \Pr(\text{e})}$$

where TP, TN, FP, and FN denote the numbers of true positives, true negatives, false positives, and false negatives, respectively. Kappa is a metric for assessing the quality of binary classifiers. Pr (e) is an estimate of the probability of a correct prediction by chance. It is calculated as:

$$\Pr(e) = \frac{(\text{TP} + \text{FN})(\text{TP} + \text{FP}) + (\text{TP} + \text{FN})(\text{TP} + \text{FP})}{(\text{TP} + \text{FN} + \text{FP} + \text{TN})^2}$$

The coverage is the proportion of test molecules with at least one nearest neighbour that meets the similarity criterion. The coverage is a measure of how many test compounds are within the applicability domain of a prediction model.

## RESULTS AND DISCUSSION

| | | |
|---|---|---|
| **Chemical Kingdom** | : | Organic Compounds |
| **Super Class** | : | Lipids and Lipid-like Molecules |
| **Class** | : | Fatty Acyls |
| **Subclass** | : | Fatty Acids and Conjugates |
| **IUPAC Name** | : | Hexadecanoic Acid |
| **Common Name** | : | Palmitic Acid, (PA) |
| **Synonym** | | hexadecanoic, hexadecanoic (palmitic) acid, hexadecanoic acid, hexadecanoic acid (palmitic acid), hexadecanoic acid (palmitic), hexadecanoic acid*, hexadecanoic-acid, hexadecanoicacid, n-hexadecanoic acid, n-hexadecanoic acid, palmistic acid, palmitate, palmitc acid, palmitic, palmitic acid, palmitic (hexadecanoic) acid, palmitic acid, palmitic acid (hexadecanoic acid), palmitic acids, palmitic-acid |
| **Compound CID** | : | 985 |
| **PubChem Identifier** | : | 985 |
| **ChEBI Identifier** | : | 57-10-3 |
| **CAS Identifier** | : | 57-10-3 |
| **Molecular Formula** | : | $C_{16}H_{32}O_2$ |
| **Molecular Weight** | : | 256.42g/mol |
| **Canonical SMILES** | : | CCCCCCCCCCCCCCCC(=O)O |
| **InChIKey** | : | IPCSVZSSVZVIGE-UHFFFAOYSA-N |

**Physiochemical properties of PA**

*In silico* biomolecular properties of PA is provided in Table 1. Physiochemical properties (value in parenthesis) of PA viz., melting point (61.8 °C); boiling point (351.5 °C); water solubility (0.04 mg/L (at 25 °C)); logP (7.17); logS (-6.81); Molecular weight (g/mol) (256.43); Log P (5.55); Topological polar surface area (Å2) (37.3); Number of hydrogen bond acceptors (1); Number of hydrogen bond donors (1); Number of carbon atoms (16); Number of heavy atoms (18); Number of heteroatoms (2); Number of nitrogen atoms (0); Number of sulfur atoms (0); Number of chiral carbon atoms (0); Stereochemical complexity (0); Number of sp hybridized carbon atoms (0); Number of sp2 hybridized carbon atoms (1); Number of sp3 hybridized carbon atoms (15); Shape complexity (0.94); Number of rotatable bonds (14); Number of aliphatic carbocycles (0); Number of aliphatic heterocycles (0); Number of aliphatic rings (0); Number of aromatic carbocycles (0); Number of aromatic heterocycles (0); Number of aromatic rings (0); Total number of rings (0); Number of saturated carbocycles (0); Number of saturated heterocycles (0); Number of saturated rings (0); Number of Smallest Set of Smallest Rings (SSSR) (0); Water Solubility (0.000407 mg/mL); logP (7.23); logP (6.26); logS (-5.8); pKa (Strongest Acidic) (4.95); Physiological Charge (-1); Hydrogen Acceptor Count (2); Hydrogen Donor Count (1); Polar Surface Area (37.3 Å2); Rotatable Bond Count (14); Refractivity (77.08 m3•mol-1); Polarizability (34.36 Å3); Number of Rings (0); Bioavailability (0); Rule of Five (No); Ghose Filter (No); Veber's Rule (No); MDDR-like Rule (No) respectively.

**Drug-likeness properties of PA**

Drug-likeness properties of PA (value in parenthesis) Number of Lipinski's rule of 5 violations (1); Lipinski's rule of 5 (Passed); Number of Ghose rule violations (0); Ghose rule (Passed); Veber rule (Bad); Egan rule (Good); GSK 4/400 rule (Bad); Pfizer 3/75 rule (Bad); Weighted quantitative estimate of drug-likeness (QEDw) score (0.41 ) respectively.

**ADMET properties of PA**

One of the key issues on the physiological role of PA is the preservation of a definite tissue concentration and repartition in different lipid classes, which requires a fine regulation of its metabolism[62]. In fact, distribution and metabolism of PA in tissues is normally maintained under stringent homeostatic control, while other aspects are unknown yet[63]. ADMET profile evaluated using admetSAR database for PA shows highest binding energy (Table 2). admetSAR predicted classification and regression values for PA and the results seems to have been calculated for different types of models such as blood brain barrier, human intestinal absorption, Caco2 permeability all of which showed positive results ensuring that the compound passes all the models and have no side effects on absorption. Similarly in case of metabolism, various CytochromeP450 (CYP) substrate and inhibitor models were calculated and the results show that they are Non substrate and Non-inhibitor except CYP450 1A2 Inhibitor. In terms of toxicity, it is found to be non-carcinogenic. Although some toxicity models show some negative results the regression profiles indicates that they have very low probability values[64].

Human Intestinal Absorption (+) - 0.9888; Blood Brain Barrier (+) - 0.9488; Caco-2 permeable (+) - 0.8326; P-glycoprotein substrate (Non-substrate) - 0.6321; P-glycoprotein inhibitor I (Non-inhibitor) - 0.9598; P-glycoprotein inhibitor II (Non-inhibitor) - 0.9277; Renal organic cation transporter (Non-inhibitor) - 0.9266; CYP450 2C9 substrate (Non-substrate) - 0.7886; CYP450 2D6 substrate (Non-substrate) - 0.8956; CYP450 3A4 substrate (Non-substrate) - 0.6982; CYP450 1A2 substrate (Inhibitor) - 0.8326; CYP450 2C9 inhibitor (Non-inhibitor) - 0.8808; CYP450 2D6 inhibitor (Non-inhibitor) - 0.9554; CYP450 2C19 inhibitor (Non-inhibitor) - 0.9578; CYP450 3A4 inhibitor (Non-inhibitor) - 0.9484; CYP450 inhibitory promiscuity (Low CYP Inhibitory Promiscuity) - 0.9647; Ames test (Non AMES toxic) - 0.9865; Carcinogenicity (Non-carcinogens) - 0.6452; Biodegradation (Ready biodegradable) - 0.8795; Rat acute toxicity (1.3275 $LD_{50}$, mol/kg) - Not applicable; hERG inhibition (predictor I) (Weak inhibitor) - 0.9322; hERG inhibition (predictor II) (Non-inhibitor) - 0.8868 respectively. Recently, Chowdhury et al[65]. demonstrated that exogenous exposure PA significantly increased protein expression of mTOR and current density of hERG 1a/1b channels. The increase in current is mediated by a targeted and increased expression of hERG 1b, through upregulation of protein translation (Table 2). Furthermore, PA significantly affected hERG 1a/1b channel inactivation kinetics[65].

**vNN based ADMET prediction models for PA**

The implemented Absorption, Distribution, Metabolism, Excretion and Toxicity (ADMET) prediction models, including their performance measures includes 15 models cover a diverse set of ADMET endpoints (Table 3).

| Query | Liver Toxicity | | Metabolism | | | | | | Membrane Transporters | | | Others | | | |
|---|---|---|---|---|---|---|---|---|---|---|---|---|---|---|---|
| | | | Cyp Inhibitors for | | | | | | | | | | | | |
| | DILI | Cyto-toxicity | HLM | 1A2 | 3A4 | 2D6 | 2C9 | 2C19 | BBB | P-gp Inhibitor | P-gp Substrate | hERG Blocker | MMP | AMES | MRTD (mg/day) |
| | Yes | ⊘ | ⊘ | No | No | No | No | No | ⊘ | No | No | Yes | No | No | 20 |

**Liver Toxicity**

**DILI**: Drug-induced liver injury (DILI) is one of the most frequent adverse clinical reactions and a relevant cause of morbidity and mortality. DILI has been one of the most commonly cited reasons for drug withdrawals from the market. This application predicts whether a compound could cause DILI. The dataset of 1,431 compounds was obtained from four sources used[66]. This dataset contains both pharmaceuticals and non-pharmaceuticals; a compound was classified as causing DILI if it was associated with a high risk of DILI and not if there was no such risk (Table 3).

**Cytotoxicity (HepG2)**: Cytotoxicity is the degree to which a chemical causes damage to cells. A cytotoxicity prediction model was developed using in vitro data on toxicity against HepG2 cells for 6,000 structurally diverse compounds, which was collected from ChEMBL. In developing the model, the compounds with an $IC_{50} \leq 10$ µM were considered in the in vitro assay as cytotoxic. Presence of high glucose and PA, HepG2 cells undergo severe metabolic and oxidative stress, resulting in increased ROS production, lipid, protein, and DNA damage, NF-kB-, TNF-α-, IL6-, and NO-dependent inflammatory responses, increased apoptosis, and decreased

mitochondrial function leading to a significant shift in the energy metabolism[67,68].

**Metabolism**

**HLM**: The human liver microsomal (HLM) stability assay is commonly used to identify and exclude compounds that are too rapidly metabolized. For a drug to achieve effective therapeutic concentrations in the body, it cannot be metabolized too rapidly by the liver. Compounds with a half-life of 30 min or longer in an HLM assay are considered as stable; otherwise they are considered unstable. HLM data was retrieved from the ChEMBL database, manually curated the data, and classified compounds as stable or unstable based on the reported half-life (T1/2 > 30 min was considered stable, and T1/2 < 30 min unstable (Table 3). The final dataset contained 3,654 compounds. Of these, as much as 2,313 were classified as stable and 1,341 as unstable[69].

**Cytochrome P450 enzyme (CYP) inhibition**: CYPs constitute a superfamily of proteins that play an important role in the metabolism and detoxification of xenobiotics[70]. In vitro data derived from five main drug-metabolizing CYPs—1A2, 3A4, 2D6, 2C9, and 2C19 were used to develop CYP inhibition models. CYP inhibitors were retrieved from PubChem and classified a compound with an $IC_{50} \leq 10$ μM for an enzyme as an inhibitor of the enzyme. Predictions for the following enzymes: CYP1A2, CYP3A4, CYP2D6, CYP2C9, and CYP2C19 have been provided (Table 3).

**Membrane Transporters**

**BBB**: The blood-brain barrier (BBB) is a highly selective barrier that separates the circulating blood from the central nervous system[46]. VNN-based BBB model has been developed, using 352 compounds whose BBB permeability values (log BB) were obtained from the literature respectively. Compounds with log BB values of less than −0.3 and greater than +0.3 were classified as BBB non-permeable and permeable (Table 3).

**Pgp Substrates and Inhibitors**: P-glycoprotein (Pgp) is an essential cell membrane protein that extracts many foreign substances from the cell. Cancer cells often overexpress Pgp, which increases the efflux of chemotherapeutic agents from the cell and prevents treatment by reducing the effective intracellular concentrations of such agents - a phenomenon known as multidrug resistance[58]. For this reason, identifying compounds that can either be transported out of the cell by Pgp (substrates) or impair Pgp function (inhibitors) is of great interest. Models to predict both Pgp substrates and Pgp inhibitors were developed. The Pgp substrate dataset contained of measurements of 422 substrates and 400 non-substrates. To generate a large Pgp inhibitor dataset and both the datasets were combined and removed duplicates to form a combined dataset consisting of training set of 1,319 inhibitors and 937 non-inhibitors (Table 3).

**hERG (Cardiotoxicity)**: The human ether-à-go-go-related gene (hERG) codes for a potassium ion channel involved in the normal cardiac repolarization activity of the heart. Drug-induced blockade of hERG function can cause long QT syndrome, which may result in arrhythmia and death[65]. As much as 282 known hERG blockers from the literature were retrieved known hERG blockers from the literature and classified compounds with an $IC_{50}$ cut-off value of 10 μM or less as blockers. A set of 404 compounds with IC50 values greater than 10 μM were collected from ChEMBL and classified them as non-blockers (Table 3).

**MMP (Mitochondrial Toxicity)**: Given the fundamental role of mitochondria in cellular energetics and oxidative stress, mitochondrial dysfunction has been implicated in cancer, diabetes, neurodegenerative disorders, and cardiovascular diseases. A largest dataset of chemical-induced changes in mitochondrial membrane potential (MMP), was used based on the assumption that a compound that causes mitochondrial dysfunction is also likely to reduce the MMP[11]. A vNN-based MMP prediction model was developed using 6,261 compounds collected from a previous study that screened a library of 10,000 compounds (~8,300 unique chemicals) at 15 concentrations, each in triplicate, to measure changes in the MMP in HepG2 cells. The study found that 913 compounds decreased the MMP, whereas 5,395 compounds had no effect (Table 3).

**Mutagenicity (Ames test)**: Mutagens are chemicals that cause abnormal genetic mutations leading to cancer. A common way to assess a chemical's mutagenicity is the Ames test[71]. A prediction model was developed using a literature dataset of 6,512 compounds, of which 3,503 were Ames-positive (Table 3).

**MRTD**: The Maximum Recommended Therapeutic Dose (MRTD) is an estimated upper daily dose that is safe[72]. A prediction model was developed based on a dataset of MRTD values publically disclosed by the FDA, mostly of single-day oral doses for an average adult with a body weight of 60 kg, for 1,220 compounds (most of which are small organic drugs). Organometallics, high-molecular weight polymers were excluded (>5,000 Da), nonorganic chemicals, mixtures of chemicals, and very small molecules (<100 Da). An external test set of 160 compounds collected by the FDA was used for validation. The total dataset for the model contained 1,185 compounds. The predicted MRTD value is reported in mg/day unit based upon an average adult weighing 60 kg (Table 3).

**Predicted human target protein associations**

TARGET (PROBABILITY); Fatty acid binding protein adipocyte (0.9359); Peroxisome proliferator-activated receptor alpha (0.9359); Fatty acid binding protein muscle (0.9359); Fatty acid binding protein epidermal (0.9359); Peroxisome proliferator-activated receptor delta (0.9359); Fatty acid binding protein intestinal (0.9359); Free fatty acid receptor 1 (0.5982); Solute carrier family 22 member 6 (0.2079); Dual specificity phosphatase Cdc25A (0.1988); 11-beta-hydroxysteroid dehydrogenase 1 (0.1534); Aldo-keto reductase family 1 member B10 (0.1262); DNA polymerase beta (0.1080); Vitamin D receptor (0.0899); Bile acid receptor FXR (0.0899); Histone lysine demethylase PHF8 (0.0899); UDP-glucuronosyltransferase 2B7 (0.0899); Cytochrome P450 19A1 (0.0899); Corticosteroid binding globulin (0.0899); Testis-specific androgen-binding protein (0.0899); Estradiol 17-beta-dehydrogenase 3 (0.0899); Glucose-6-phosphate 1-dehydrogenase (0.0899); GABA-B receptor (0.0899); Prostanoid EP2 receptor (0.0899); Lysine-specific demethylase 2A (0.0899); Lysine-specific demethylase 5C (0.0899); G-protein coupled bile acid receptor 1 (0.0899); Niemann-Pick C1-like protein 1 (0.0626); GABA A receptor alpha-2/beta-2/gamma-2 (0.0626); Protein farnesyltransferase (0.0626); Androgen Receptor (0.0626); Hydroxyacid oxidase 1 (0.0536); Prostanoid FP receptor (0.0536); Protein-tyrosine phosphatase 1B (0.0536); 11-beta-hydroxysteroid dehydrogenase 2 (0.0536); Glutathione S-transferase kappa 1 (0.0536); Leukotriene A4 hydrolase (0.0536); Carbonic anhydrase II (0.0536); Carbonic anhydrase I (0.0536); Nuclear receptor subfamily 0 group B (0.0536); CDC45-related protein (0.0536); Leukocyte common antigen (0.0536); Peroxisome proliferator-activated receptor (0.0536); Cytochrome P450 26A1 (0.0536); Retinoid X receptor alpha (0.0536); Retinoic acid receptor gamma

(0.0536); Retinoic acid receptor beta (0.0536); Retinoic acid receptor alpha (0.0536); Anandamide amidohydrolase (0.0536); Telomerase reverse transcriptase (0.0536); Fatty acid-binding protein, liver (0.0536); Cytochrome P450 26B1 (0.0536); Retinoid X receptor gamma (0.0536); G-protein coupled receptor 120 (0.0536); Voltage-gated calcium channel alpha2 (0.0536); Retinoid X receptor beta (0.0536); Monocarboxylate transporter 1 (0.0536); Arachidonate 15-lipoxygenase (0.0536); Arachidonate 12-lipoxygenase (0.0536); Prostanoid EP4 receptor (0.0536); Glycine receptor subunit alpha-1 (0.0536); Epoxide hydratase (0.0536); Multidrug resistance-associated protein 1 (0.0536); P-glycoprotein 1 (0.0536); Neuronal acetylcholine receptor protein alpha-7 (0.0536); Cytosolic phospholipase A2 (0.0536); Prostaglandin E synthase (0.0536); Acyl-CoA desaturase (0.0536); SUMO-activating enzyme (0.0536); Metabotropic glutamate receptor 5 (0.0536); Plasminogen (0.0536); Serotonin 2b (5-HT2b) receptor (0.0536); Nuclear receptor ROR-beta (0.0536); MAP kinase ERK2 (0.0536); Nuclear receptor ROR-alpha (0.0536); GPCR 44 (0.0536); Intercellular adhesion molecule (ICAM-1), Integrin (0.0536); Thromboxane A2 receptor (0.0000); Hepatocyte nuclear factor 4-alpha (0.0000) respectively (**Table** 4; Fig. 1).

## CONCLUSION

PBNPs from wild plants still remain an ideal storehouse of phyto pharmaceutical compounds[73]. Data obtain in the present study depict that PA could be a potential NS5B polymerase inhibitor besides other ADMET properties predicted for PA indicate that it is non-carcinogenic and biodegradable. Finally, the results may have some implications in elucidating the molecular mechanisms that critically regulates pathophysiological metabolic events in the regulations of hyperglycemia/ hyperlipidemia-induced complications associated with diabesity and CVD and provide better understanding to identify key molecular targets for the therapeutic management of PA induced metabolic disorders.

## REFERENCES


1. Gunstone FD, Harwood JL. The lipid handbook with CD-ROM. CRC press; 2007 Mar 13 https://doi.org/10.1201/9781420009675

2. Hill K, Höfer R. Natural fats and oils. Sustainable solutions for modern economies. The Royal Society of Chemistry. 2009 Nov 20:167-237. https://doi.org/10.1039/9781847552686-00167

3. Carta G, Murru E, Banni S, Manca C. Palmitic acid: physiological role, metabolism and nutritional implications. Frontiers in physiology. 2017 Nov 8; 8:902 https://doi.org/10.3389/fphys.2017.00902

4. Jahromi KG, Koochi ZH, Kavoosi G, Shahsavar A. Manipulation of fatty acid profile and nutritional quality of Chlorella vulgaris by supplementing with citrus peel fatty acid. Scientific Reports. 2022 May 17; 12(1):1-1 https://doi.org/10.1038/s41598-022-12309-y

5. Kien CL, Bunn JY, Ugrasbul F. Increasing dietary palmitic acid decreases fat oxidation and daily energy expenditure-. The American journal of clinical nutrition. 2005 Aug 1; 82(2):320-6 https://doi.org/10.1093/ajcn/82.2.320

6. Donnelly KL, Smith CI, Schwarzenberg SJ, Jessurun J, Boldt MD, Parks EJ. Sources of fatty acids stored in liver and secreted via lipoproteins in patients with nonalcoholic fatty liver disease. The Journal of clinical investigation. 2005 May 2; 115(5):1343-51 https://doi.org/10.1172/JCI23621

7. Trombetta A, Togliatto G, Rosso A, Dentelli P, Olgasi C, Cotogni P, Brizzi MF. Increase of Palmitic acid concentration impairs endothelial progenitor cell and bone marrow-derived progenitor cell bioavailability: role of the STAT5/PPARγ transcriptional complex. Diabetes. 2013 Apr 1; 62(4):1245-57 https://doi.org/10.2337/db12-0646

8. Cheng L, Yu Y, Szabo A, Wu Y, Wang H, Camer D, Huang XF. Palmitic acid induces central leptin resistance and impairs hepatic glucose and lipid metabolism in male mice. The Journal of nutritional biochemistry. 2015 May 1; 26(5):541-8 https://doi.org/10.1016/j.jnutbio.2014.12.011

9. Yuan L, Mao Y, Luo W, Wu W, Xu H, Wang XL, Shen YH. Palmitic acid dysregulates the Hippo-YAP pathway and inhibits angiogenesis by inducing mitochondrial damage and activating the cytosolic DNA sensor cGAS-STING-IRF3 signaling mechanism. Journal of Biological Chemistry. 2017 Sep 8; 292(36):15002-15 https://doi.org/10.1074/jbc.M117.804005

10. Fatima S, Hu X, Gong RH, Huang C, Chen M, Wong HL, Bian Z, Kwan HY. Palmitic acid is an intracellular signaling molecule involved in disease development. Cellular and Molecular Life Sciences. 2019 Jul; 76(13):2547-57 https://doi.org/10.1007/s00018-019-03092-7

11. Binker-Cosen MJ, Richards D, Oliver B, Gaisano HY, Binker MG, Cosen-Binker LI. Palmitic acid increases invasiveness of pancreatic cancer cells AsPC-1 through TLR4/ROS/NF-κB/MMP-9 signaling pathway. Biochemical and biophysical research communications. 2017 Feb 26; 484(1):152-8 https://doi.org/10.1016/j.bbrc.2017.01.051

12. Lin L, Ding Y, Wang Y, Wang Z, Yin X, Yan G, Zhang L, Yang P, Shen H. Functional lipidomics: Palmitic acid impairs hepatocellular carcinoma development by modulating membrane fluidity and glucose metabolism. Hepatology. 2017 Aug; 66(2):432-48 https://doi.org/10.1002/hep.29033

13. Ng YW, Say YH. Palmitic acid induces neurotoxicity and gliatoxicity in SH-SY5Y human neuroblastoma and T98G human glioblastoma cells. PeerJ. 2018 Apr 26; 6:e4696 https://doi.org/10.7717/peerj.4696

14. Hernández-Cáceres MP, Cereceda K, Hernández S, Li Y, Narro C, Rivera P, Silva P, Ávalos Y, Jara C, Burgos P, Toledo-Valenzuela L. Palmitic acid reduces the autophagic flux in hypothalamic neurons by impairing autophagosome-lysosome fusion and endolysosomal dynamics. Molecular & cellular oncology. 2020 Sep 2; 7(5):1789418 https://doi.org/10.1080/23723556.2020.1789418

15. Hernández-Cáceres MP, Cereceda K, Hernández S, Li Y, Narro C, Rivera P, Silva P, Ávalos Y, Jara C, Burgos P, Toledo-Valenzuela L. Palmitic acid reduces the autophagic flux in hypothalamic neurons by impairing autophagosome-lysosome fusion and endolysosomal dynamics. Molecular & cellular oncology. 2020 Sep 2; 7(5):1789418 https://doi.org/10.1080/23723556.2020.1789418

16. Padayachee B, Baijnath H. An overview of the medicinal importance of Moringaceae. Journal of Medicinal Plants Research. 2012; 6(48):5831-9.

17. Kou X, Li B, Olayanju JB, Drake JM, Chen N. Nutraceutical or pharmacological potential of Moringa oleifera Lam. Nutrients. 2018; 10(3):343. https://doi.org/10.3390/nu10030343

18. Saini RK, Sivanesan I, Keum YS. Phytochemicals of Moringa oleifera: a review of their nutritional, therapeutic and industrial significance. 3 Biotech. 2016; 6(2):1-4. https://doi.org/10.1007/s13205-016-0526-3

19. Rathnayake ARMHA, Navaratne SB, Uthpala TGG Moringa oleifera plant and the nutritional and medicinal properties of Moringa oleifera leaves Trends Pros. Process. Hort. Crops 2019; 251-268

20. Luqman S, Srivastava S, Kumar R, Maurya AK, Chanda D. Experimental assessment of Moringa oleifera leaf and fruit for its antistress, antioxidant, and scavenging potential using in vitro and in vivo assays. Evidence-Based Complementary and Alternative Medicine. 2012; 2012. https://doi.org/10.1155/2012/519084

21. Jung IL. Soluble extract from Moringa oleifera leaves with a new anticancer activity. PloS one. 2014; 9(4):e95492. https://doi.org/10.1371/journal.pone.0095492

22. Manavalan N, Boopathi NM, Raveendran M. Medicinal and Therapeutic Properties of Moringa. In The Moringa Genome 2021 (pp. 31-39). Springer, Cham. https://doi.org/10.1007/978-3-030-80956-0_4

23. Abalaka ME, Daniyan SY, Oyeleke SB, Adeyemo SO. The antibacterial evaluation of Moringa oleifera leaf extracts on selected bacterial pathogens. Journal of Microbiology research. 2012; 2(2):1-4. https://doi.org/10.5923/j.microbiology.20120202.01

24. Patel P, Patel N, Patel D, Desai S, Meshram D. Phytochemical analysis and antifungal activity of Moringa oleifera. International Journal of Pharmacy and Pharmaceutical Sciences. 2014; 6(5):144-7.

25. Boopathi NM, Abubakar BY. Botanical Descriptions of Moringa spp. In The Moringa Genome 2021 (pp. 11-20). Springer, Cham. https://doi.org/10.1007/978-3-030-80956-0_2

26. Kalaimathi RV, Krishnaveni K, Murugan M, Basha AN, Gilles AP, Kandeepan C, Senthilkumar N, Mathialagan B, Ramya S, Ramanathan L, Jayakumararaj R. ADMET informatics of Tetradecanoic acid (Myristic Acid) from ethyl acetate fraction of Moringa oleifera leaves. Journal of Drug Delivery and Therapeutics. 2022 Aug 20; 12(4-S):101-11. https://doi.org/10.22270/jddt.v12i4-S.5533

27. Kandeepan C, Sabitha M, Parvathi K, Senthilkumar N, Ramya S, Boopathi NM, Jayakumararaj R. Phytochemical Screening, GCMS Profile, and In-silico properties of Bioactive Compounds in Methanolic Leaf Extracts of Moringa oleifera. Journal of Drug Delivery and Therapeutics. 2022 Mar 15; 12(2):87-99. https://doi.org/10.22270/jddt.v12i2.5250

28. Meena R, Prajapati SK, Nagar R, Porwal O, Nagar T, Tilak VK, Jayakumararaj R, Arya RK, Dhakar RC. Application of Moringa oleifera in Dentistry. Asian Journal of Dental and Health Sciences. 2021 Dec 25; 1(1):10-3.

29. Murugan M, Krishnaveni K, Sabitha M, Kandeepan C, Senthilkumar N, Loganathan T, Pushpalatha GL, Pandiarajan G, Ramya S, Jayakumararaj R. In silico Target Class Prediction and Probabilities for Plant Derived Omega 3 Fatty Acid from Ethyl Acetate Fraction of Moringa oleifera Leaf Extract. Journal of Drug Delivery and Therapeutics. 2022 May 20; 12(3):124-37. https://doi.org/10.22270/jddt.v12i3.5352

30. Parvathi K, Kandeepan C, Sabitha M, Senthilkumar N, Ramya S, Boopathi NM, Ramanathan L, Jayakumararaj R. In-silico Absorption, Distribution, Metabolism, Elimination and Toxicity profile of 9, 12, 15-Octadecatrienoic acid (ODA) from Moringa oleifera. Journal of Drug Delivery and Therapeutics. 2022 Apr 15; 12(2-S):142-50. https://doi.org/10.22270/jddt.v12i2-S.5289

31. Van De Waterbeemd H, Gifford E. ADMET in silico modelling: towards prediction paradise?. Nature reviews Drug discovery. 2003 Mar; 2(3):192-204. https://doi.org/10.1038/nrd1032

32. Guan L, Yang H, Cai Y, Sun L, Di P, Li W, Liu G, Tang Y. ADMET-score-a comprehensive scoring function for evaluation of chemical drug-likeness. Medchemcomm. 2019; 10(1):148-57. https://doi.org/10.1039/C8MD00472B

33. Bose PP, Chatterjee U, Hubatsch I, Artursson P, Govender T, Kruger HG, Bergh M, Johansson J, Arvidsson PI. In vitro ADMET and physicochemical investigations of poly-N-methylated peptides designed to inhibit Aβ aggregation. Bioorganic & medicinal chemistry. 2010; 18(16):5896-902. https://doi.org/10.1016/j.bmc.2010.06.087

34. Ramya S, Loganathan T, Chandran M, Priyanka R, Kavipriya K, Pushpalatha GL, Aruna D, Abraham GC, Jayakumararaj R. ADME-Tox profile of Cuminaldehyde (4-Isopropylbenzaldehyde) from Cuminum cyminum seeds for potential biomedical applications. Journal of Drug Delivery and Therapeutics. 2022 Apr 15; 12(2-S):127-41. https://doi.org/10.22270/jddt.v12i2-S.5286

35. Kandeepan C, Kalaimathi RV, Jeevalatha A, Basha AN, Ramya S, Jayakumararaj R. In-silico ADMET Pharmacoinformatics of Geraniol (3, 7-dimethylocta-trans-2, 6-dien-1-ol)-acyclic monoterpene alcohol drug from Leaf Essential Oil of Cymbopogon martinii from Sirumalai Hills (Eastern Ghats), INDIA. Journal of Drug Delivery and Therapeutics. 2021 Aug 15; 11(4-S):109-18. https://doi.org/10.22270/jddt.v11i4-S.4965

36. Krishnaveni K, Sabitha M, Murugan M, Kandeepan C, Ramya S, Loganathan T, Jayakumararaj R. vNN model cross validation towards Accuracy, Sensitivity, Specificity and kappa performance measures of β-caryophyllene using a restricted-unrestricted applicability domain on Artificial Intelligence & Machine Learning approach based in-silico prediction. Journal of Drug Delivery and Therapeutics. 2022 Feb 22; 12(1-S):123-31. https://doi.org/10.22270/jddt.v12i1-S.5222

37. Loganathan T, Barathinivas A, Soorya C, Balamurugan S, Nagajothi TG, Ramya S, Jayakumararaj R. Physicochemical, Druggable, ADMET Pharmacoinformatics and Therapeutic Potentials of Azadirachtin-a Prenol Lipid (Triterpenoid) from Seed Oil Extracts of Azadirachta indica A. Juss. Journal of Drug Delivery and Therapeutics. 2021 Sep 15; 11(5):33-46. https://doi.org/10.22270/jddt.v11i5.4981

38. Ramya S, Murugan M, Krishnaveni K, Sabitha M, Kandeepan C, Jayakumararaj R. In-silico ADMET profile of Ellagic Acid from Syzygium cumini: A Natural Biaryl Polyphenol with Therapeutic Potential to Overcome Diabetic Associated Vascular Complications. Journal of Drug Delivery and Therapeutics. 2022 Jan 15; 12(1):91-101. https://doi.org/10.22270/jddt.v12i1.5179

39. Ramya S, Neethirajan K, Jayakumararaj R. Profile of bioactive compounds in Syzygium cumini-a review. J. Pharm. Res. 2012 Aug; 5(8):4548-53.

40. Ramya S, Soorya C, Pushpalatha GG, Aruna D, Loganathan T, Balamurugan S, Abraham GC, Ponrathy T, Kandeepan C, Jayakumararaj R. Artificial Intelligence and Machine Learning approach based in-silico ADME-Tox and Pharmacokinetic Profile of α-Linolenic acid from Catharanthus roseus (L.) G. Don. Journal of Drug Delivery and Therapeutics. 2022 Apr 15; 12(2-S):96-109. https://doi.org/10.22270/jddt.v12i2-S.5274

41. Sabitha M, Krishnaveni K, Murugan M, Basha AN, Pallan GA, Kandeepan C, Ramya S, Jayakumararaj R. In-silico ADMET predicated Pharmacoinformatics of Quercetin-3-Galactoside, polyphenolic compound from Azadirachta indica, a sacred tree from Hill Temple in Alagarkovil Reserve Forest, Eastern Ghats, INDIA. Journal of Drug Delivery and Therapeutics. 2021 Oct 15; 11(5-S):77-84. https://doi.org/10.22270/jddt.v11i5-S.5026

42. Kalaimathi RV, Jeevalatha A, Basha AN, Kandeepan C, Ramya S, Loganathan T, Jayakumararaj R. In-silico Absorption, Distribution, Metabolism, Elimination and Toxicity profile of Isopulegol from Rosmarinus officinalis. Journal of Drug Delivery and Therapeutics. 2022 Jan 15; 12(1):102-8. https://doi.org/10.22270/jddt.v12i1.5188

43. Mabkhot YN, Alatibi F, El-Sayed NN, Al-Showiman S, Kheder NA, Wadood A, Rauf A, Bawazeer S, Hadda TB. Antimicrobial activity of some novel armed thiophene derivatives and petra/osiris/molinspiration (POM) analyses. Molecules. 2016; 21(2):222. https://doi.org/10.3390/molecules21020222

44. Beetge E, du Plessis J, Müller DG, Goosen C, van Rensburg FJ. The influence of the physicochemical characteristics and pharmacokinetic properties of selected NSAID's on their transdermal absorption. International journal of Pharmaceutics. 2000; 193(2):261-4. https://doi.org/10.1016/S0378-5173(99)00340-3

45. Hauser AS, Attwood MM, Rask-Andersen M, Schiöth HB, Gloriam DE. Trends in GPCR drug discovery: new agents, targets and indications. Nature reviews Drug discovery. 2017; 16(12):829-42. https://doi.org/10.1038/nrd.2017.178

46. Daina A, Michielin O, Zoete V. SwissADME: a free web tool to evaluate pharmacokinetics, drug-likeness and medicinal chemistry friendliness of small molecules. Scientific reports. 2017; 7(1):1-3. https://doi.org/10.1038/srep42717

47. Guan L, Yang H, Cai Y, Sun L, Di P, Li W, Liu G, Tang Y. ADMET-score-a comprehensive scoring function for evaluation of chemical drug-likeness. Medchemcomm. 2019; 10(1):148-57. https://doi.org/10.1039/C8MD00472B

48. Hubatsch I, Ragnarsson EG, Artursson P. Determination of drug permeability and prediction of drug absorption in Caco-2

monolayers. Nature protocols. 2007 Sep; 2(9):2111-9. https://doi.org/10.1038/nprot.2007.303

49. Radchenko EV, Dyabina AS, Palyulin VA, Zefirov NS. Prediction of human intestinal absorption of drug compounds. Russian Chemical Bulletin. 2016; 65(2):576-80. https://doi.org/10.1007/s11172-016-1340-0

50. Alam A, Kowal J, Broude E, Roninson I, Locher KP. Structural insight into substrate and inhibitor discrimination by human P-glycoprotein. Science. 2019; 363(6428):753-6. https://doi.org/10.1126/science.aav7102

51. Daina A, Zoete V. A boiled-egg to predict gastrointestinal absorption and brain penetration of small molecules. ChemMedChem. 2016; 11(11):1117-21. https://doi.org/10.1002/cmdc.201600182

52. Liao M, Jaw-Tsai S, Beltman J, Simmons AD, Harding TC, Xiao JJ. Evaluation of in vitro absorption, distribution, metabolism, and excretion and assessment of drug-drug interaction of rucaparib, an orally potent poly (ADP-ribose) polymerase inhibitor. Xenobiotica. 2020; 50(9):1032-42. https://doi.org/10.1080/00498254.2020.1737759

53. Cheng F, Li W, Zhou Y, Shen J, Wu Z, Liu G, Lee PW, Tang Y. admetSAR: a comprehensive source and free tool for assessment of chemical ADMET properties. 2012; 3099-3105. https://doi.org/10.1021/ci300367a

54. Schyman, P., R. Liu, V. Desai, and A. Wallqvist. vNN web server for ADMET predictions. Frontiers in Pharmacology. 2017 December 4; 8:889. https://doi.org/10.3389/fphar.2017.00889

55. Liu, R., G. Tawa, and A. Wallqvist. Locally weighted learning methods for predicting dose-dependent toxicity with application to the human maximum recommended daily dose. Chemical Research in Toxicology. 2012; 25(10):2216-2226. https://doi.org/10.1021/tx300279f

56. Liu, R., and A. Wallqvist. Merging applicability domains for in silico assessment of chemical mutagenicity. Journal of Chemical Information and Modeling. 2014; 54(3):793-800.

https://doi.org/10.1021/ci500016v

57. Liu, R., P. Schyman, and A. Wallqvist. Critically assessing the predictive power of QSAR models for human liver microsomal stability. Journal of Chemical Information and Modeling. 2015; 55(8):1566-1575. https://doi.org/10.1021/acs.jcim.5b00255

58. Schyman, P., R. Liu, and A. Wallqvist. Using the variable-nearest neighbor method to identify P-glycoprotein substrates and inhibitors. ACS Omega. 2016; 1(5):923-929. https://doi.org/10.1021/acsomega.6b00247

59. Muehlbacher, M., G. Spitzer, K. Liedl, J. Kornhuber. Qualitative prediction of blood-brain barrier permeability on a large and refined dataset. Journal of Computer-Aided Molecular Design. 2011; 25:1095. https://doi.org/10.1007/s10822-011-9478-1

60. Naef R. A generally applicable computer algorithm based on the group additivity method for the calculation of seven molecular descriptors: heat of combustion, logPO/W, logS, refractivity, polarizability, toxicity and logBB of organic compounds; scope and limits of applicability. Molecules. 2015; 20(10):18279-18351 https://doi.org/10.3390/molecules201018279

61. Xu, Y., Z. Dai, F. Chen, S. Gao, J. Pei, and L. Lai. Deep learning for drug-induced liver injury. 2015; 55(10):2085-2093. https://doi.org/10.1021/acs.jcim.5b00238

62. Carta G, Murru E, Banni S, Manca C. Palmitic acid: physiological role, metabolism and nutritional implications. Frontiers in physiology. 2017 Nov 8; 8:902 https://doi.org/10.3389/fphys.2017.00902

63. Rampersaud AM, Dunk CE, Lye SJ, Renaud SJ. Palmitic acid induces inflammation in placental trophoblasts and impairs their migration toward smooth muscle cells through plasminogen activator inhibitor-1. Molecular human reproduction. 2020 Nov 1; 26(11):850-65 https://doi.org/10.1093/molehr/gaaa061

64. Balavignesh V, Srinivasan E, Ramesh Babu NG, Saravanan N. Molecular docking study ON NS5B polymerase of hepatitis c virus by screening of volatile compounds from Acacia concinna and ADMET prediction. Int J Pharm Life Sci. 2013 Apr;4:2548-58

65. Chowdhury MK, Aromolaran KA, Do J, Aromolaran AS. Regulation of hERG 1a/1b channels through the mTOR complex 1 signaling pathway in lipotoxic heart. Biophysical Journal. 2022 Feb 11; 121(3):303 https://doi.org/10.1016/j.bpj.2021.11.1234

66. Thakkar S, Chen M, Fang H, Liu Z, Roberts R, Tong W. The Liver Toxicity Knowledge Base (LKTB) and drug-induced liver injury (DILI) classification for assessment of human liver injury. Expert review of gastroenterology & hepatology. 2018 Jan 2; 12(1):31-8. https://doi.org/10.1080/17474124.2018.1383154

67. Alnahdi A, John A, Raza H. Augmentation of glucotoxicity, oxidative stress, apoptosis and mitochondrial dysfunction in HepG2 cells by palmitic acid. Nutrients. 2019 Aug 22; 11(9):1979 https://doi.org/10.3390/nu11091979

68. Yoshitomi S, Ikemoto K, Takahashi J, Miki H, Namba M, Asahi S. Establishment of the transformants expressing human cytochrome P450 subtypes in HepG2, and their applications on drug metabolism and toxicology. Toxicology in Vitro. 2001 Jun 1; 15(3):245-56. https://doi.org/10.1016/S0887-2333(01)00011-X

69. Lee PH, Cucurull-Sanchez L, Lu J, Du YJ. Development of in silico models for human liver microsomal stability. Journal of computer-aided molecular design. 2007; 21(12):665-73. https://doi.org/10.1007/s10822-007-9124-0

70. Pelkonen O, Turpeinen M, Hakkola J, Honkakoski P, Hukkanen J, Raunio H. Inhibition and induction of human cytochrome P450 enzymes: current status. Archives of toxicology. 2008; 82(10):667-715. https://doi.org/10.1007/s00204-008-0332-8

71. Stead AG, Hasselblad V, Creason JP, Claxton L. Modeling the Ames test. Mutation Research/Environmental Mutagenesis and Related Subjects. 1981 Feb 1; 85(1):13-27. https://doi.org/10.1016/0165-1161(81)90282-X

72. Matthews EJ, Kruhlak NL, Benz RD, Contrera JF. Assessment of the health effects of chemicals in humans: I. QSAR estimation of the maximum recommended therapeutic dose (MRTD) and no effect level (NOEL) of organic chemicals based on clinical trial data1. Current drug discovery technologies. 2004 Jan 1; 1(1):61-76. https://doi.org/10.2174/1570163043484789

73. Nazar S, Jeyaseelan M, Jayakumararaj R. Local Health Traditions, Cultural Reflections and Ethno-taxonomical Information on Wild Edible Fruit Yielding Medicinal Plants in Melur Region of Madurai District, TamilNadu, India. Journal of Drug Delivery and Therapeutics. 2022 Jun 15; 12(3):138-57. https://doi.org/10.22270/jddt.v12i3.5405

**Table 1 *In silico* biomolecular properties of PA**

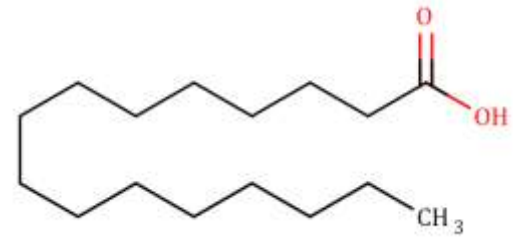


| Molecular Properties | Calculated Values |
|---|---|
| **miLogP** | 7.06 |
| **TPSA** | 37.30 |
| **Natoms** | 18 |
| **MW** | 256.43 |
| **nON** | 2 |
| **nOHNH** | 1 |
| **Nviolations** | 1 |
| **Nrotb** | 14 |
| **volume** | 291.42 |
| **Biological Properties** | **Bioactivity Scores** |
| **GPCR ligand** | 0.02 |
| **Ion channel modulator** | 0.06 |
| **Kinase inhibitor** | -0.33 |
| **Nuclear receptor ligand** | 0.08 |
| **Protease inhibitor** | -0.04 |
| **Enzyme inhibitor** | 0.18 |

**Table 2 Summary of Physicochemical, Druggability & ADMET Properties of PA**

| **Physicochemical Properties** | | |
|---|---|---|
| Molecular weight | | 256.43 g/mol |
| LogP | | 5.55 |
| LogD | | 3.84 |
| LogSw | | -5.02 |
| Number of stereocenters | | 0 |
| Stereochemical complexity | | 0.000 |
| Fsp3 | | 0.938 |
| Topological polar surface area | | 37.30 Å$^2$ |
| Number of hydrogen bond donors | | 1 |
| Number of hydrogen bond acceptors | | 1 |
| Number of smallest set of smallest rings (SSSR) | | 0 |
| Size of the biggest system ring | | 0 |
| Number of rotatable bonds | | 14 |
| Number of rigid bonds | | 1 |
| Number of charged groups | | 1 |
| Total charge of the compound | | -1 |
| Number of carbon atoms | | 16 |
| Number of heteroatoms | | 2 |
| Number of heavy atoms | | 18 |
| Ratio between the number of non-carbon atoms and the number of carbon atoms | | 0.13 |
| **Druggability Properties** | | |
| Lipinski's rule of 5 violations | | 1 |
| Veber rule | | Good |
| Egan rule | | Good |
| Oral PhysChem score (Traffic Lights) | | 4 |
| GSK's 4/400 score | | Good |
| Pfizer's 3/75 score | | Bad |
| Weighted quantitative estimate of drug-likeness (QEDw) score | | 0.334 |
| Solubility | | 1688.61 |
| Solubility Forecast Index | | Good |
| **ADMET Properties Property** | **Value** | |
| Human Intestinal Absorption | HIA+ | 0.989 |
| Blood Brain Barrier | BBB+ | 0.949 |
| Caco-2 permeable | Caco2+ | 0.833 |
| P-glycoprotein substrate | Non-substrate | 0.632 |
| P-glycoprotein inhibitor I | Non-inhibitor | 0.960 |
| P-glycoprotein inhibitor II | Non-inhibitor | 0.928 |
| CYP450 2C9 substrate | Non-substrate | 0.789 |
| CYP450 2D6 substrate | Non-substrate | 0.896 |
| CYP450 3A4 substrate | Non-substrate | 0.698 |
| CYP450 1A2 inhibitor | Inhibitor | 0.833 |
| CYP450 2C9 inhibitor | Non-inhibitor | 0.881 |
| CYP450 2D6 inhibitor | Non-inhibitor | 0.955 |
| CYP450 2C19 inhibitor | Non-inhibitor | 0.958 |
| CYP450 3A4 inhibitor | Non-inhibitor | 0.948 |
| CYP450 inhibitory promiscuity | Low CYP Inhibitory Promiscuity | 0.965 |
| Ames test | Non AMES toxic | 0.987 |
| Carcinogenicity | Non-carcinogens | 0.645 |
| Biodegradation | Ready biodegradable | 0.880 |
| Rat acute toxicity | 1.328 LD50, mol/kg | NA |
| hERG inhibition (predictor I) | Weak inhibitor | 0.932 |
| hERG inhibition (predictor II) | Non-inhibitor | 0.887 |

**Table 3 Performance measures of vNN models in 10-fold cross validation using a restricted or unrestricted applicability domain**

| Model | Data[a] | $d_0$[b] | h[c] | Accuracy | Sensitivity | Specificity | kappa | R[d] | Coverage |
|---|---|---|---|---|---|---|---|---|---|
| DILI | 1427 | 0.60 | 0.50 | 0.71 | 0.70 | 0.73 | 0.42 | | 0.66 |
| | | 1.00 | 0.20 | 0.67 | 0.62 | 0.72 | 0.34 | | 1.00 |
| Cytotox (hep2g) | 6097 | 0.40 | 0.20 | 0.84 | 0.88 | 0.76 | 0.64 | | 0.89 |
| | | 1.00 | 0.20 | 0.84 | 0.73 | 0.89 | 0.62 | | 1.00 |
| HLM | 3219 | 0.40 | 0.20 | 0.81 | 0.72 | 0.87 | 0.59 | | 0.91 |
| | | 1.00 | 0.20 | 0.81 | 0.70 | 0.87 | 0.57 | | 1.00 |
| CYP1A2 | 7558 | 0.50 | 0.20 | 0.90 | 0.70 | 0.95 | 0.66 | | 0.75 |
| | | 1.00 | 0.20 | 0.89 | 0.61 | 0.95 | 0.60 | | 1.00 |
| CYP2C9 | 8072 | 0.50 | 0.20 | 0.91 | 0.55 | 0.96 | 0.54 | | 0.76 |
| | | 1.00 | 0.20 | 0.90 | 0.44 | 0.96 | 0.46 | | 1.00 |
| CYP2C19 | 8155 | 0.55 | 0.20 | 0.87 | 0.64 | 0.93 | 0.58 | | 0.76 |
| | | 1.00 | 0.20 | 0.86 | 0.52 | 0.94 | 0.50 | | 1.00 |
| CYP2D6 | 7805 | 0.50 | 0.20 | 0.89 | 0.61 | 0.94 | 0.57 | | 0.75 |
| | | 1.00 | 0.20 | 0.88 | 0.52 | 0.95 | 0.51 | | 1.00 |
| CYP3A4 | 10373 | 0.50 | 0.20 | 0.88 | 0.76 | 0.92 | 0.68 | | 0.78 |
| | | 1.00 | 0.20 | 0.88 | 0.69 | 0.93 | 0.64 | | 1.00 |
| BBB | 353 | 0.60 | 0.20 | 0.90 | 0.94 | 0.86 | 0.80 | | 0.61 |
| | | 1.00 | 0.10 | 0.82 | 0.88 | 0.75 | 0.64 | | 1.00 |
| Pgp Substrate | 822 | 0.60 | 0.20 | 0.79 | 0.80 | 0.79 | 0.58 | | 0.66 |
| | | 1.00 | 0.20 | 0.73 | 0.73 | 0.74 | 0.47 | | 1.00 |
| Pgp Inhibitor | 2304 | 0.50 | 0.20 | 0.85 | 0.91 | 0.73 | 0.66 | | 0.76 |
| | | 1.00 | 0.10 | 0.81 | 0.86 | 0.74 | 0.61 | | 1.00 |
| hERG | 685 | 0.70 | 0.70 | 0.84 | 0.84 | 0.83 | 0.68 | | 0.80 |
| | | 1.00 | 0.20 | 0.82 | 0.82 | 0.83 | 0.64 | | 1.00 |
| MMP | 6261 | 0.50 | 0.40 | 0.89 | 0.64 | 0.94 | 0.61 | | 0.69 |
| | | 1.00 | 0.20 | 0.87 | 0.52 | 0.94 | 0.50 | | 1.00 |
| AMES | 6512 | 0.50 | 0.40 | 0.82 | 0.86 | 0.75 | 0.62 | | 0.79 |
| | | 1.00 | 0.20 | 0.79 | 0.82 | 0.75 | 0.57 | | 1.00 |
| MRTD[e] | 1184 | 0.60 | 0.20 | | | | | 0.79 | 0.69 |
| | | 1.00 | 0.20 | | | | | 0.74 | 1.00 |

**Table 4 In silico target predication and the probability for PA**

| TARGET | COMMON.NAME | UNIPROT.ID | TARGET CLASS | PROBABILITY |
|---|---|---|---|---|
| Fatty acid binding protein adipocyte | FABP4 | P15090 | Fatty acid BPF | 0.935895337456 |
| Peroxisome proliferator-activated receptor alpha | PPARA | Q07869 | Nuclear receptor | 0.935895337456 |
| Fatty acid binding protein muscle | FABP3 | P05413 | Fatty acid BPF | 0.935895337456 |
| Fatty acid binding protein epidermal | FABP5 | Q01469 | Fatty acid BPF | 0.935895337456 |
| Peroxisome proliferator-activated receptor delta | PPARD | Q03181 | Nuclear receptor | 0.935895337456 |
| Fatty acid binding protein intestinal | FABP2 | P12104 | Fatty acid BPF | 0.935895337456 |
| Free fatty acid receptor 1 | FFAR1 | O14842 | Family A GPCR | 0.598213027933 |
| Solute carrier family 22 member 6 | SLC22A6 | Q4U2R8 | Electrochemtransporter | 0.207865841523 |
| Dual specificity phosphatase Cdc25A | CDC25A | P30304 | Phosphatase | 0.198808518053 |
| 11-beta-hydroxysteroid dehydrogenase 1 | HSD11B1 | P28845 | Enzyme | 0.153377072466 |
| Aldo-keto reductase family 1 member B10 | AKR1B10 | O60218 | Enzyme | 0.126154249845 |
| DNA polymerase beta | POLB | P06746 | Enzyme | 0.108018050868 |
| Vitamin D receptor | VDR | P11473 | Nuclear receptor | 0.0898720672475 |
| Bile acid receptor FXR | NR1H4 | Q96RI1 | Nuclear receptor | 0.0898720672475 |
| Histone lysine demethylase PHF8 | PHF8 | Q9UPP1 | Eraser | 0.0898720672475 |
| UDP-glucuronosyltransferase 2B7 | UGT2B7 | P16662 | Enzyme | 0.0898720672475 |
| Cytochrome P450 19A1 | CYP19A1 | P11511 | Cytochrome P450 | 0.0898720672475 |
| Corticosteroid binding globulin | SERPINA6 | P08185 | Secreted protein | 0.0898720672475 |
| Testis-specific androgen-binding protein | SHBG | P04278 | Secreted protein | 0.0898720672475 |
| Estradiol 17-beta-dehydrogenase 3 | HSD17B3 | P37058 | Enzyme | 0.0898720672475 |
| Glucose-6-phosphate 1-dehydrogenase | G6PD | P11413 | Enzyme | 0.0898720672475 |
| GABA-B receptor | GABBR1 | Q9UBS5 | Family C GPCR | 0.0898720672475 |
| Prostanoid EP2 receptor | PTGER2 | P43116 | Family A GPCR | 0.0898720672475 |
| Lysine-specific demethylase 2A | KDM2A | Q9Y2K7 | Eraser | 0.0898720672475 |
| Lysine-specific demethylase 5C | KDM5C | P41229 | Eraser | 0.0898720672475 |
| G-protein coupled bile acid receptor 1 | GPBAR1 | Q8TDU6 | Family A GPCR | 0.0898720672475 |
| Niemann-Pick C1-like protein 1 | NPC1L1 | Q9UHC9 | Other membrane protein | 0.0626219668353 |
| GABA A receptor alpha-2/beta-2/gamma-2 | GABRA2 | P47869 | Ligand-gated channel | 0.0626219668353 |
| Protein farnesyltransferase | FNTA | P49354 | Enzyme | 0.0626219668353 |
| Androgen Receptor | AR | P10275 | Nuclear receptor | 0.0626219668353 |
| Hydroxyacid oxidase 1 | HAO1 | Q9UJM8 | Enzyme | 0.0535560755162 |
| Prostanoid FP receptor | PTGFR | P43088 | Family A GPCR | 0.0535560755162 |
| Protein-tyrosine phosphatase 1B | PTPN1 | P18031 | Phosphatase | 0.0535560755162 |
| 11-beta-hydroxysteroid dehydrogenase 2 | HSD11B2 | P80365 | Enzyme | 0.0535560755162 |
| Glutathione S-transferase kappa 1 | GSTK1 | Q9Y2Q3 | Enzyme | 0.0535560755162 |
| Leukotriene A4 hydrolase | LTA4H | P09960 | Protease | 0.0535560755162 |
| Carbonic anhydrase II | CA2 | P00918 | Lyase | 0.0535560755162 |
| Carbonic anhydrase I | CA1 | P00915 | Lyase | 0.0535560755162 |

| | | | | |
|---|---|---|---|---|
| Nuclear receptor subfamily 0 group B | NR0B2 | Q15466 | Nuclear receptor | 0.0535560755162 |
| CDC45-related protein | CDC45 | O75419 | Other nuclear protein | 0.0535560755162 |
| Leukocyte common antigen | PTPRC | P08575 | Enzyme | 0.0535560755162 |
| Peroxisome proliferator-activated receptor | PPARG | P37231 | Nuclear receptor | 0.0535560755162 |
| Cytochrome P450 26A1 | CYP26A1 | O43174 | Cytochrome P450 | 0.0535560755162 |
| Retinoic acid receptor gamma | RARG | P13631 | Nuclear receptor | 0.0535560755162 |
| Retinoic acid receptor beta | RARB | P10826 | Nuclear receptor | 0.0535560755162 |
| Retinoic acid receptor alpha | RARA | P10276 | Nuclear receptor | 0.0535560755162 |
| Anandamide amidohydrolase | FAAH | O00519 | Enzyme | 0.0535560755162 |
| Telomerase reverse transcriptase | TERT | O14746 | Enzyme | 0.0535560755162 |
| Fatty acid-binding protein, liver | FABP1 | P07148 | Fatty acid BPF | 0.0535560755162 |
| Cytochrome P450 26B1 | CYP26B1 | Q9NR63 | Cytochrome P450 | 0.0535560755162 |
| Retinoid X receptor gamma | RXRG | P48443 | Nuclear receptor | 0.0535560755162 |
| G-protein coupled receptor 120 | FFAR4 | Q5NUL3 | Family A GPCR | 0.0535560755162 |
| Voltage-gated calcium channel alpha2 | CACNA2D1 | P54289 | Calcium channel | 0.0535560755162 |
| Retinoid X receptor beta | RXRB | P28702 | Nuclear receptor | 0.0535560755162 |
| Monocarboxylate transporter 1 | SLC16A1 | P53985 | Electro transporter | 0.0535560755162 |
| Arachidonate 15-lipoxygenase | ALOX15 | P16050 | Enzyme | 0.0535560755162 |
| Arachidonate 12-lipoxygenase | ALOX12 | P18054 | Enzyme | 0.0535560755162 |
| Prostanoid EP4 receptor | PTGER4 | P35408 | Family A GPCR | 0.0535560755162 |
| Glycine receptor subunit alpha-1 | GLRA1 | P23415 | Ligand-gated channel | 0.0535560755162 |
| Epoxide hydratase | EPHX2 | P34913 | Protease | 0.0535560755162 |
| Multidrug resistance-associated protein 1 | ABCC1 | P33527 | PAT | 0.0535560755162 |
| P-glycoprotein 1 | ABCB1 | P08183 | Active transporter | 0.0535560755162 |
| Neuronal acetylcholine receptor protein alpha-7 | CHRNA7 | P36544 | Ligand-gated channel | 0.0535560755162 |
| Cytosolic phospholipase A2 | PLA2G4A | P47712 | Enzyme | 0.0535560755162 |
| Prostaglandin E synthase | PTGES | O14684 | Enzyme | 0.0535560755162 |
| Acyl-CoA desaturase | SCD | O00767 | Enzyme | 0.0535560755162 |
| SUMO-activating enzyme | SAE1 | Q9UBE0 | Enzyme | 0.0535560755162 |
| Metabotropic glutamate receptor 5 | GRM5 | P41594 | Family C GPCR | 0.0535560755162 |
| Plasminogen | PLG | P00747 | Protease | 0.0535560755162 |
| Serotonin 2b (5-HT2b) receptor | HTR2B | P41595 | Family A GPCR | 0.0535560755162 |
| Nuclear receptor ROR-beta | RORB | Q92753 | Nuclear receptor | 0.0535560755162 |
| MAP kinase ERK2 | MAPK1 | P28482 | Kinase | 0.0535560755162 |
| Nuclear receptor ROR-alpha | RORA | P35398 | Nuclear receptor | 0.0535560755162 |
| GPCR 44 | PTGDR2 | Q9Y5Y4 | Family A GPCR | 0.0535560755162 |
| Intercellular adhesion molecule (ICAM-1), Integrin | ITGAL | P20701 | Membrane receptor | 0.0535560755162 |
| Thromboxane A2 receptor | TBXA2R | P21731 | Family A GPCR | 0.0 |
| Hepatocyte nuclear factor 4-alpha | HNF4A | P41235 | Unclassified protein | 0.0 |

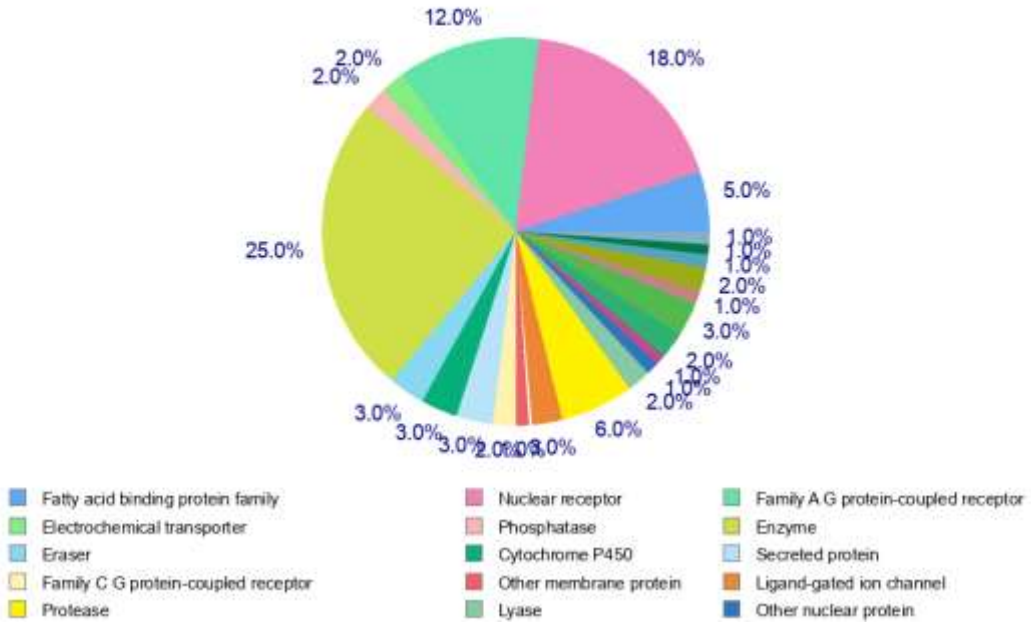


**Figure 1 Percentage functional targets for PA**